Effect of Moisture on Full Scale Pavement Distress

José Aguiar-Moya[1], Edgar Camacho-Garita[2], Eliécer Arias-Barrantes [3], Luis Loría-Salazar[4]
([1] LanammeUCR, San José, Costa Rica, jose.aguiar@ucr.ac.cr)
([2] LanammeUCR, San José, Costa Rica, edgar.camachogarita@ucr.ac.cr)
([3] LanammeUCR, San José, Costa Rica, eliecer.arias@ucr.ac.cr)
([4] LanammeUCR, San José, Costa Rica, luis.loriasalazar@ucr.ac.cr)

ABSTRACT

The effect of moisture is fundamental in determining pavement response. The effect becomes more important when high levels of moisture and precipitation are present. This is the case of tropical regions such as Costa Rica where high precipitation rates, high variability in water table levels, and materials that are highly susceptible to the previous are common.

The results indicate that when comparing the performance of pavement sections that are subjected to near saturation conditions, the bearing capacity of the pavement structure can be as low as 5% of that associated to the same structure but with little moisture. The damage in the saturated pavement sections is greatly accelerated due to pumping of fines from the subgrade and the subbase.

All the pavement layers are affected by loading (decrease or increase in layer module). Furthermore, the effect of moisture is greater in the cohesive soils and contaminated granular materials. Finally, it is the relatively stiffer layers (i.e. HMA and CTB layers) the ones that are more susceptible to a higher deterioration rate, particularly under saturated or near saturated conditions.

Keywords: Moisture, accelerated pavement test, layer module, water table levels, subgrade.

1. INTRODUCTION

Costa Rica, as is the case of many other Tropical countries, is subject to changes in microclimate in very short distances, rapid and aggressive atmospheric changes, and high precipitation levels. The previous is worsened because of high loads travelling at low speeds, expansive soils and drainage systems that are insufficient or nonexistent to meet the demand of the rainy season.

Moisture damage can occur at the interface between the mastic (mixture of asphalt binder and mineral filler) and aggregate surface (adhesive failure) or within the mastic structure itself (cohesive failure). However, several other factors would also influence the moisture susceptibility such as the addition of a binder modifier, liquid anti-strip agent, or hydrated lime [1]. It has also been reported that an increase in the pH of the water at the asphalt binder and aggregate surface interface has an important effect on the weakening of the adhesion bond between the two materials [2].

A literature review [3] showed that at least five different mechanisms of failure are associated to moisture damage and stripping, and might occur individually or simultaneously: detachment, displacement, spontaneous emulsification, pore pressure, and hydraulic scouring. Detachment occurs when a thin layer of water displaces the complete asphalt film from the aggregate surface. This is a result of lower free surface energy of water as compared to the asphalt binder, resulting in a higher wet-ability of the aggregate [3-4].

By itself, moisture damage is not a type of distress but a conditioning process which will result in the appearance of one or more different distress types that can be load related such as fatigue cracking and rutting, or thermal stress related such as transverse or block cracking [5-6]. Consequently, the effect of moisture damage on the HMA layers can be quantified by means of changes in layer stiffness [7].

It has been generally shown that the presence of moisture in the granular and cohesive layers below the HMA layer results in a reduction in bearing strength, and therefore a reduction in pavement service life [8-11]. The issue of moisture is more relevant still when considering that the balance of water in the pavement structure is constantly changing [12]

In general, the effect of moisture on material stiffness is nonlinear and is highly dependent on the construction process (eg. Compaction of granular or cohesive layers and gradation) and can result in a significant increase in permanent deformation [13-14]. Furthermore, moisture content changes continuously since the construction phase due to climatic variations such as precipitation, variations in ground water table, and freeze-thaw cycles.

Specially in the case of fine-grained unbound materials, the state of saturation can significantly affect the material response due to pore pressure [15]. Increases in the fine content, plasticity index, and methylene blue values result in materials that are more susceptible to moisture changes [16].

Moisture affects the unbound materials by altering its properties: resilient modulus, shear strength, cohesion, susceptibility to volumetric changes, and erosion. Therefore, adequate knowledge of moisture content should be required to properly model material performance. Typically, moisture content has been related to rainfall [17].

The objective of this study was to evaluate the effect of moisture on pavement performance based on full scale accelerated pavement testing (APT) results for two distinct pavement structures.

2. TEST SECTIONS

The test sections used in the analysis are part of the initial set of experiments performed at PaveLab in Costa Rica, and correspond to 4 structures that were constructed by March 2012, HVS trafficking on the sections began in July 2013 using a dual 11R22-5 tire, with 90 psi inflation pressure, applying a standardized load between 40 kN and 80 kN. The objective of this set of experiments consisted in the structural comparison of typical conditions in the Country: use of granular vs cement-treated bases (CTB), and thin vs thick HMA layers.

The top layer consists of an asphalt concrete (AC) mixture with nominal maximum aggregate size of 19.0 mm with an optimum binder content of 4.9% by total weight of mixture. The CTB was designed to withstand 35 kg/cm2 with an optimum cement content of 1.7% by volume of aggregate and with a maximum density of 2013 kg/m^3. The base material and granular subbase were placed at a maximum density of 2217 kg/m^3 with an optimum moisture content of 8.6%. The subbase material had a CBR of 95%. Finally, the subgrade material (MH, A-7-5) was constructed for a maximum density of 1056 kg/m3 with an optimum moisture content of 52% (typical moisture content in Costa Rica) and CBR of 6.6%. Both the subgrade and subbase material properties are uniform for all test sections.

The control of the water table was performed by a gravity operated water distribution system that was constructed adjacent to the test pit. The overall design of the test pits is based on experience at other APT facilities [18].

Table 1. Construction Test Tracks in-place Properties.

Properties \ Section	**AC1**	**AC2**	**AC3**	**AC4**
AC Thickness (H1), cm	6.1	6.3	13.2	13.2
Base Thickness (H2), cm	21.9	21.2	31.0	24.9
Subbase Thickness (H3), cm	30.1	30.1	30.1	30.1

3. INSTRUMENTATION

HVS onboard instrumentation records the applied load, tire pressure and temperature, position and velocity of the load carriage. The HVS was further equipped with a laser profiler that can be used to create a three-dimensional profile of the section and a road surface deflectometer (RSD) to obtain deflection at the test section. Finally, a moisture gauge was also installed on each pavement sections that were to be evaluated under saturated or wet condition.

Data of the 3D profile and RSD is collected on daily basis, after 20,000 load repetitions.

4. RESULTS

To observe how saturation of the underlying layers affects pavement performance, laser profile measurements were recorded throughout the tests to monitor the evolution of the parameter in time. The previous allowed for 3D distributions of rutting and IRI within the test sections. Stiffness was also monitored throughout the test using the RSD. The recorded data was later processed to perform back-calculation of the layer module.

Backcalculation was performed based on Odemark-Boussineq theory while considering the non-linear behaviour of the subgrade [19]. The resilient modulus values that are presented are based on 580 back-calculation runs for the different structures at different time intervals resulting in 2300 individual layer stiffness values.

A significant difference in loads required to achieve failure when comparing a pavement section under dry and saturated condition was observed. Figure 3 and 4 shows the change in HMA layer stiffness during the APT tests. In terms of ESALs, it can be determined that the AC2-Dry section outlasted the AC2-Wet section by 21 times: 9.40 vs 0.45 MESALs respectively.

Furthermore, towards the end of the service life under wet conditions, the HMA layers exhibit a significant decrease in resilient modulus as measured by the RSD: change from an initial stiffness of 3500 MPA vs 439 MPa prior to failure; 12 percent of the initial capacity. The results for the AC1 section under dry and wet conditions is not shown since the failure mechanism differed: non-significant changes to HMA modulus since most of the damage occurred in the CTB layer.

It is important to note that the failure mechanisms between the dry and wet conditions are considerably different. In the case of dry pavement structures, failure was related to a decrease in stiffness of some layers, minor cracking, and permanent deformation. In the case of the partially saturated pavement structures, the previous failure conditions were also observed but at considerably higher intensity. Significant pumping of fines was also observed in the latter case.

When comparing how the different moisture conditions can affect the behaviour of the different layers within the pavement structure, it can be noted that moisture mainly affects the stiffness of the subgrade. The previous can be expected to the material properties (higher plasticity and susceptibility to volumetric changes). In the case of the AC2 test sections, reductions in subgrade stiffness between 4 and 14 times when comparing the dry and saturated conditions. In the case of the AC1 sections, differences of up to 24 times were recorded when comparing the 2 moisture conditions (Figure 2).

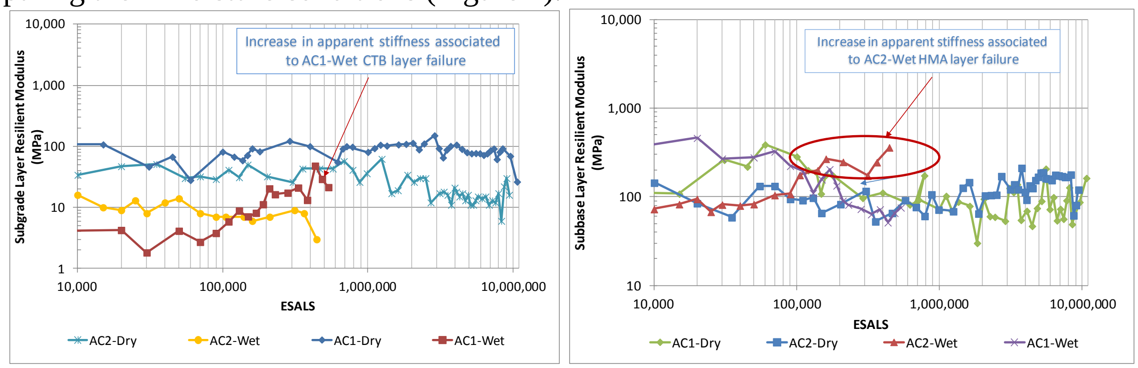

Figure 1 and 2 Change in subgrade stiffness and change in subbase stiffness with loading.

Figure 2 shows the evolution of the granular subbase modulus during the test. It can be observed that prior to loading; the test sections have a similar stiffness (200 – 300 MPa). However, towards the end of the test and prior to failure, the pavement sections that are saturated show an increase in stiffness that can be attributed to the decreased capacity of the HMA layer and the nonlinear behaviour of the material, resulting in a considerable change to the stress distribution throughout the pavement structure prior to failure.

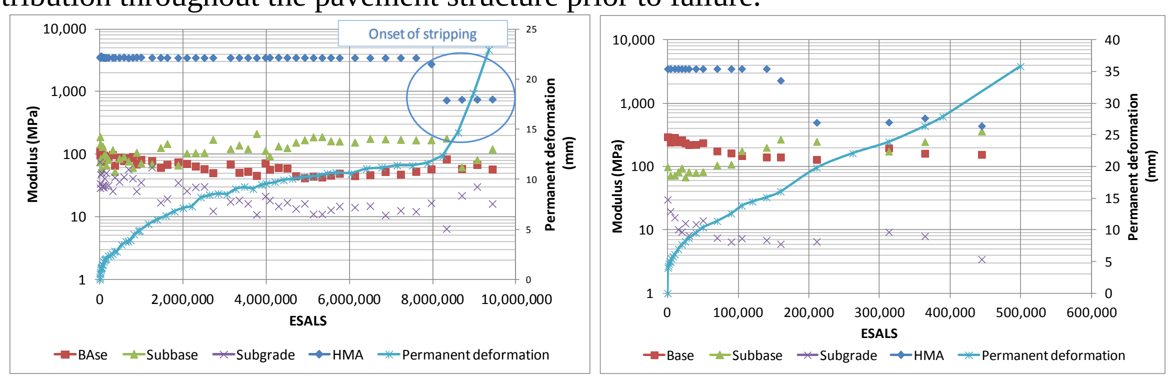

Figure 3 and 4 Change in layer stiffness and permanent deformation for section AC2-Dry and section AC2-Wet.

Figure 3 and 4 shows a summary of the change in stiffness for the different layers, as well as the permanent deformation for a test section. It can be observed that the reduction in stiffness of the subgrade layer was considerable throughout the test: change from initial stiffness of 47 MPa to 12 MPa at failure. The previous can be associated to damage in the material which was evaluated under constant conditions. This can also be indicative of insufficient capacity of the pavement structure. An increase in the modulus of the subbase layer can be observed (stress hardening). The effect can also be attributed to a loading conditioning previous to the deflection measurements.

Each load step is performed to accelerate the damage and to increase the number of ESAL applications to the pavement section. However, it is important to highlight that this loading pattern is not random but has been equally applied to all evaluated pavement sections. The load procedure was developed so that when a pavement structure reaches a stable deterioration stage, the increase in the load (10 kN each increase) accelerates the damage process.

Towards the end of the service life of a particular pavement section, two processes can be clearly identified and related: 1) the loss in resilient modulus of the HMA layer which highly correlates with 2) the increased rate of distress (i.e. increase in permanent deformation and IRI). For example, the largest increase in permanent deformation occurs during the application of the last loads: 100% increase in deformation during the final 10% applied ESALs.

Section AC2-Wet exhibit similar trends in terms of stiffness (Figure 4). However, the changes occurred during a completely different time interval. Even though sections AC2-Dry and AC2-Wet are structurally identical, the presence of moisture resulted in the latter only having the 5% of the structural capacity of the former (dry condition).

Because of the previous, the permanent deformation pattern for the AC2-Wet section is different than that of AC2-Dry. Figure 4 shows that after the initial consolidation process, the permanent deformation follows a relatively linear trend, with a deformation rate of approximately 6 mm per 100,000 ESALs. The behaviour is different than that of section AC2-Dry that exhibits the typical 3 stage deformation process. In the case of AC1-Dry, the evolution of permanent deformation was very similar to that of AC2-Dry.

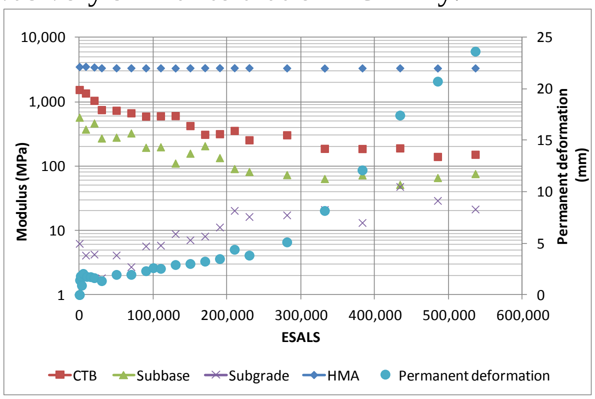

Figure 5 Change in layer stiffness and permanent deformation for section AC1-Wet.

Figure 5 shows the evolution of permanent deformation for the AC1-Wet section. The section includes a CTB layer which greatly decelerated the onset of permanent deformation during the initial 250,000 ESAL applications. However, after the previous threshold, when the CTB layer stiffness begins to reduce significantly, a clear increase in deformation rate can be observed, concluding in the failure of the section based on deformation and IRI criteria.

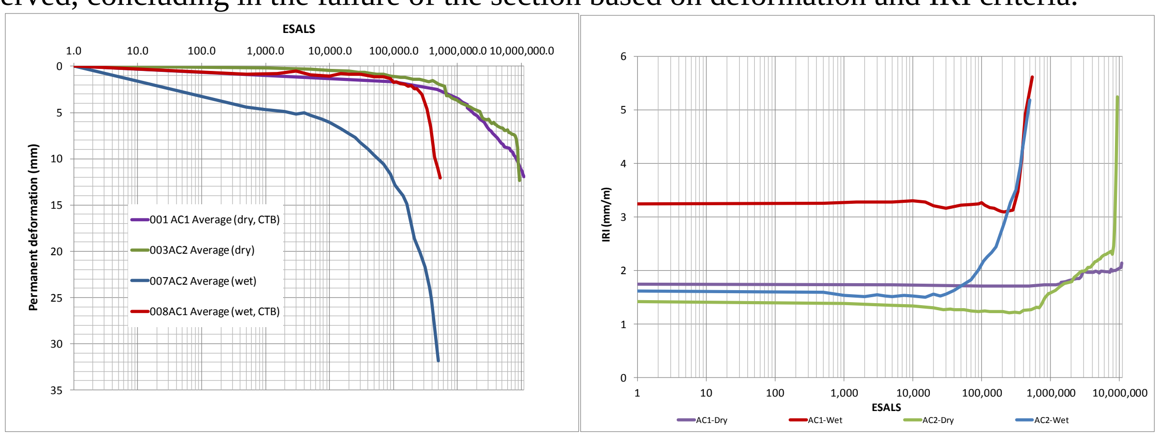

Figure 6 and 7 Change in permanent deformation and Change in IRI

Figure 6 shows how permanent deformation increased for the different test sections. The data is presented in logarithmic scale to allow for a simpler visual comparison of the distress evolution considering pavement sections in dry and saturated conditions.

As in the case of change in stiffness, the pavement sections that were evaluated under dry condition reach the failure deformation at a considerably slower rate than their saturated counterparts.

The profile lasers that were used in the study are very similar to those used for measuring the longitudinal profile of roads at highway speeds, and consequently allows for estimating IRI by means of the quarter-car vehicle math. A limitation associated to the IRI estimation is that the length of the section is 6 m, and within this distance the effective measuring distance of the lasers is 5.1 m.

The IRI results for the analyzed sections are shown on Figure 7. The figure shows that during initial loading, there is a slight improvement in IRI associated to material rearrangement and post-compaction.

As expected, the change in IRI highly correlates to the changes in material stiffness that was previously observed, as well to the increase in permanent deformation associated to loading.

5. CONCLUSIONS

In the case of the analyzed pavements structures, it was shown that saturation or partial saturation of the underlying layers significantly affects the durability and stability of the pavement structure. Capacity in terms of ESALs to failure under wet conditions ranged from 4.71% to 5.00% for the AC2 and AC1 sections respectively, with respect to the dry sections.

Except for AC2-Wet, all the sections showed a typical 3 stage permanent deformation evolution: post compaction, constant deformation rate, and finally higher deformation and stripping. In the case of the AC2-Wet section (granular base), the deformation rate was rather constant: 6 mm per 100,000 ESAL applications, and did not reach the tertiary deformation stage.

In the case of the AC2 (granular base) sections, it was observed that towards the end of their service life, the resilient modulus of the HMA layer had decreased to a value between 12% and 20% of the initial modulus.

In the case of the sections with a CTB layer, it was observed that the resilient modulus drop to approximately 50% of the initial stiffness after very few load applications (2% and 5% of the ESALs required for failure for the AC1-Dry and AC1-Wet sections respectively). At failure, the stiffness of the CTB layer had reduced significantly: 10% of initial modulus in the case of the AC1-Wet section.

The apparent increase in stiffness of the subbase and subgrade that was observed is currently under analysis by means of multilayer linear elastic and finite element analysis. However, as discussed in the paper, the phenomena are expected to be related to the nonlinear behaviour of the cohesive subgrade soil.

Finally, the APT experiments to analyze the effect of moisture are expected to continue while modifying the thickness of the different layers, the materials, and the construction process with the aim of collecting the required information to calibrate layer response and performance models that can adequately account for moisture conditions present in tropical regions.

6. REFERENCES

[1] Howson, J., Masad, E.A., Bhasin, A., Castelo, V., Arambula, E., Lytton, R, and Little, D. System for the Evaluation of Moisture Damage Using Fundamental Material Properties. Report FHWA/TX-07/0-4524-1. Texas, 2007.

[2] Scott, J.A.N. Adhesion and Disbonding Mechanisms of Asphalt Used in Highway Construction and Maintenance. Proceedings of the Association of Asphalt Paving Technologists, Vol. 47, pp 19-24 Minessota, 1982.

[3] Tarrer, A.R., and Wagh, V. The Effect of the Physical and Chemical Characteristics of the Aggregate on Bonding. Report SHRP-A/UIR-91-507. Washington, D.C., 1991.

[4] Majidzadra, K., and Brovold, F.N. State of the Art: Effect of Water on Bitumen-Aggregate Mixtures. Highway Research Board Special Rept. 98. Washington, D.C., 1968.

[5] Little, D.N., Epps, J.A., and Sebaaly, P.E. The Benefits of hydrated lime in hot mix asphalt. National Lime Association. 2006.

[6] Sebaaly, P.E. Comparison of Lime and Liquid Additives on the Moisture Damage of Hot Mix Asphalt Mixtures. National Lime Association. 2007.

[7] Aguiar-Moya, J.P., Torres-Linares, P., Camacho-Garita, E., Leiva-Villacorta, F., and Loría-Salazar, L.G. Development of IRI Models Based on APT Data. The Roles of Accelerated Pavement Testing in Pavement Sustainability, pp 799-813. 2016.

[8] Hussain, J., Wilson, D.J., Henning, T., and Alabaster, D. What happens when it rains? Performance of unbound flexible pavements in accelerated pavement testing. Road and Transport Research Vol. 20, Issue 4, pp. 3-15. 2011.

[9] Toros, U., and Hiltunen, D. Effects of moisture and time on stiffness of unbound aggregate base coarse materials. Transportation Research Record 2059, pp. 41–51. 2008.

[10] Ekblad, J., and Isacsson, U. Influence of water on resilient properties of coarse granular materials. Road Materials and Pavement Design, vol. 7, pp. 369–404. 2006.

[11] Ekblad, J., and Isacsson, U. Influence of water and mica content on resilient properties of coarse granular materials. International Journal of Pavement Engineering, Vol. 9, pp. 215–27. 2008.

[12] Zapata, C.E., Perera, Y.Y., and Houston, W.N. Matric suction prediction model in new AASHTO mechanistic-empirical pavement design guide. Transportation Research Record 2101, pp. 53–62. 2009.

[13] Huurman, R., and Molenaar, A.A.A. Permanent deformation in flexible pavements with unbound base courses. Transportation Research Record 1952, pp. 31–8. 2006.

[14] Chandra, D., Chua, K.M., and Lytton, R.L. Effects of temperature and moisture on the load response of granular base course material in thin pavements. Transportation Research Record 1252, pp. 33–41. 1989.

[15] Salour, F., Erlingsson, S., and Zapata, C.E. Modelling resilient modulus seasonal variation of silty sand subgrade soils with matric suction control. Canadian Geotechnical Journal 51, pp. 1413-1422. 2014.

[16] Caicedo, B., Coronado, O., Fleureau, J.M., Gomes, A. Resilient Behaviour of non Standard Unbound Granular Materials. Road Materials And Pavement Design, Vol. 10 , Issue 2, pp. 287-312. 2009.

[17] Zapata, C., and Salim, R. Impact of environmental site location and groundwater table depth on thickness of flexible airfield pavements. Transportation Research Record 2282, pp. 22-33. 2012.

[18] Hugo, F., Epps Martin, A.L. Significant Findings from Full-Scale Accelerated Pavement Testing. NCHRP Synthesis 325. Washington, D.C. 2004.
[19] Ullidtz, P. Pavement Analysis, Development in Civil Engineering, Vol.19, Amsterdam, the Netherlands. 1987.